–

Power diagram based algorithm for the facility location and capacity acquisition problem with dense demand

Yuyou YAO, Wenming WU, Gaofeng ZHANG, Benzhu XU, Liping ZHENG(✉)

School of Computer Science and Information Engineering, Hefei University of Technology, Hefei 230601, China

Abstract The facility Location and Capacity Acquisition Problem (LCAP) is one of the most widely used groups in operations research and has been extensively used for healthcare, emergency center locating, etc. The allocation of customers to facilities is mainly based on the Euclidean distance between customers and facilities in previous studies. However, in addition to the distance, the attraction of facilities also depends on some features, such as the scale and service level in the retail store locating. To this end, a continuous model for the LCAP with dense demand is proposed in this paper, where in addition to the distance, these features, characterized by the weighting coefficients, are taken into consideration, which help to describe the real attraction process of facilities. Furthermore, a power diagram based algorithm is developed to solve the LCAP, in which the allocation decisions are determined based on the power diagram. On the one hand, the gradient descent method is applied to optimize the weighting coefficients of facilities. On the other hand, Lloyd's method is employed to update the location of each facility. Computational results demonstrate the effectiveness of our proposed method.

Keywords Location-allocation problem, facility location, capacity acquisition, power diagram, dense demand

1 Introduction

The Location-Allocation Problem (LAP) is one of the classic problems in operations research, which is widely used in practical applications, such as the blood supply chains, healthcare, clustering problems, and the emergency center locating, etc. Cooper [1] first introduces the basic concepts of the LAP, which locates a set of new facilities such that the transportation cost from facilities to customers is minimized. Recently, a more generalized version of the LAP has been introduced, called the facility Location and Capacity Acquisition Problem (LCAP), which is essential to real-word firms, e.g. the retail store locating, cloudlet placement for mobile edge computing [2], and automotive service firms locating [3], which mainly involves the issues of where to build facilities, how much capacity to acquire, and which parts of the market region each facility should serve.

There are roughly two categories of methods to investigate the LCAP models. The first one is the discrete model, and the other one is the continuous model. For the former model, probability distribution functions, such as Poisson distribution and Normal distribution, are used to estimate the demands of customers. Different from the former model, dense demands, represented by the approximation continuous functions, are considered in the latter model.

Existing research algorithms have certain limitations for the LCAP with continuous model. Iri et al. [4] introduce a Voronoi diagram based algorithm for the LCAP. Murat et al. [5] propose a vertex-based iterative algorithm to solve the LCAP, which requires much more time consuming as compared with the previous algorithms. However, the allocation decisions are determined based on the Euclidean distance in the above algorithms, which cannot well express the attraction process in some real-world applications. For instance, the attraction of facilities is closely related to the scale and service level of facilities in the retail store locating. Bourne et al. [6] present an iterative algorithm for the LCAP with uniform dense demand. In addition to the distance, the attraction of facilities depends on a set of features, which are characterized by the weighting coefficients [7]. However, due to the diverse demands of customers, these demands are often randomly distributed, so modeling demands as a general dense demand is more preferable in practical applications, instead of uniform dense demand [5].

Therefore, we propose a power diagram based iterative method for the LCAP with general dense demand, in which the gradient descent method is employed to update the weight-

E-mail: zhenglp@hfut.edu.cn

ing coefficients of facilities, and Lloyd's method is applied to optimize the location of each facility. The main contributions of this work are summarized as follows:

1) introducing a continuous model for the LCAP, in which the transportation cost is a non-linear function of the Euclidean distance.
2) employing the power diagrams to determine the allocation decisions with general dense demand.
3) developing a novel iterative method to solve the LCAP with dense demand, which is fast and efficient.

The remainder of this paper is organized as follows. Section 2 briefly reviews the related work. Section 3 introduces the continuous model for the LCAP. The allocation method and iterative algorithm are presented in Section 4. Section 5 illustrates some computational results and some conclusions are given in Section 6.

2 Related work

In recent years, many studies have been conducted on the LAP and its variants, which can be classified into two categories. The first one is the discrete model, and the other one is the continuous model. For the former model, probability distribution functions, such as Poisson distribution and Normal distribution, are used to estimate the demands of customers. Different from the former model, dense demands, represented by the approximation continuous functions, are considered in the latter model. Table 1 presents a classification of the existing methods of the LAP and its variants.

Table 1 A classification of the existing method of the LAP and its variants.

Methods	Type	Model	Capacity
Fernandez et al. [8]	LAP	DM	UC
Lin [9]	LAP	DM	UC
Li et al. [10]	LAP	DM	UC
Ankrah et al. [11]	LAP	DM	UC
Zhou et al. [12]	LAP	DM	UC
Murat et al. [5]	LCAP	CM	C
Marucheck et al. [13]	LAP	CM	UC
Wang et al. [14]	LAP	CM	UC
Yin et al. [15]	LAP	DM	C
Harris et al. [16]	LAP	DM	C
Liu et al. [17]	LAP	DM	UC
Grine et al. [18]	LAP	CM	UC
Dasci et al. [19]	LCAP	CM	UC
Iri et al. [4]	LCAP	CM	UC
Murat et al. [20]	LCAP	CM	UC
Turken et al. [21]	LAP	CM	UC

DM: Discrete model; CM: Continuous model
UC: Uncapacitated; C: Capacitated

For the discrete model, early studies model the LAP on the basis of scenarios [8]. Besides, the uncertain demands can be estimated by probability distribution, so as to achieve a more general discrete model. Lin [9] employs Poisson distribution to demonstrate these demands, while Normal distribution is applied in [10]. However, the distribution of customers may be unfixed in some practical applications, instead of fixed in the previous studies. Ankrah et al. [11] introduce the LAP with dynamic customer, in which customers move over time. Furthermore, Zhou et al. [12] model the LAP with fuzzy demands, and three types of fuzzy programming models are proposed, which can effectively solve the LAP. The optimal solution can be obtained in the previous studies with small demands, nevertheless, more time consuming is required in the computation process with the increasing of demands.

However, due to the difficulty of predicting the demands of customers in the discrete model, these demands are modeled as approximation continuous functions ("demand density functions") in other studies, which can be divided into uniform and general demand densities based on the type of demand density function. In the case of uniform dense demand, Maruchek et al. [13] consider the uniform dense demand on the rectangular regions and propose a branch-and-bound algorithm for the LAP. However, due to the diverse demands of customers, these demands are often randomly distributed, so modeling these demands as a general demand density is more preferable. Joseph et al. [22] introduce the population density patterns by both the monocentric and polycentric models, and Wang [14] proposes the two-stage LAP of multiple facilities with curved demands, and applies it to the West-to-East natural gas transmission project, which can effectively obtain the optimal solutions.

Furthermore, some researchers focus on the capacitated LAP, in which the capacities of facilities are limited. Yin et al. [15] propose a capacitated LAP model to minimize the cost of allocating facilities, and an evolutionary bi-objective approach to the capacitated facility location problem is described in [16]. However, setting the preset capacities of facilities may be difficult in practical applications, such as the retail store locating and automotive service firms locating [17], etc. Some studies turn to the uncapacitated LAP, where the capacities of facilities are limitless. Grine et al. [18] propose an effective metaheuristic algorithm for solving the uncapacitated single allocation p-hub median problem.

Recently, a more generalized version of the LAP, called the LCAP, is illustrated in [19]. Iri et al. [4] introduce a Voronoi diagram based algorithm for the LCAP, and an equivalent dynamic programming formulation that prioritizes allocation decisions is introduced in [20]. Besides, Murat et al. [5] propose a vertex-based iterative algorithm to solve the LCAP, which requires much more time consuming as compared with the previous algorithms. However, the allocation decisions are determined based on the Euclidean distance in the above algorithms. In addition to the distance, the attraction of facilities is closely related to the scale and service level of facilities in the real-world applications, such as the retail store locating, etc. Turken et al. [21] analyses the impact of factors, such as the and command-and-control and carbon tax, on the facility location decision.

3 Continuous model for the LCAP

In this section, we describe the continuous model for the LCAP in detail. Furthermore, we reformulate our model as a multi-facility locating problem.

3.1 Problem description

Consider a market region $M \subset R^2$ in the convex polygon shape, over which a large number of customers are distributed, which are modeled as a spatial density function $\rho(\mathbf{x})$. Let $\mathbf{X} = \{\mathbf{x}_i\}_{i=1}^n$ denote the coordinates of n independent facilities, where $\mathbf{x}_i = (x_i, y_i) \in M$ represents the location of i-th facility. The market region M is therefore partitioned into n disjoint subregions (called "service regions") $\mathbf{R} = \{R_i\}_{i=1}^n$, and service region R_i is assigned to the facility located at $\mathbf{x}_i$. Based on the previous studies on the LCAP, the total cost has three main components in our model: (1) the annualized fixed cost F_i, (2) the capacity acquisition cost f_i, and (3) the transportation cost C_i. A multi-objective optimization continuous model is built to find the optimal solution as follows:

$$\min_{\mathbf{X},\,\mathbf{R}} E_{LCAP} = \sum_{i=1}^{n} \{F_i + f_i + C_i\} \tag{1}$$

3.2 Fixed cost

The annualized fixed cost can be considered as the required cost before constructing a new facility, e.g. the cost of purchasing or renting, etc. Therefore, the annualized fixed cost is closely related to the location of each facility, and the annualized fixed cost of i-th facility is $F(\mathbf{x}_i) = F_i(\mathbf{x}_i)$.

3.3 Capacity acquisition cost

The capacity acquisition cost is vital characteristic in the LCAP, which can be considered as the cost of building or running the facilities. The total demand within the service region R_i can be represented by $m_i = \int_{R_i} \rho(\mathbf{x}) d\mathbf{x}$. Based on the description in [20], the capacity acquisition cost $f_i = f(\mathbf{x}_i, m_i)$ of the i-th facility is assumed to depend on both the location $\mathbf{x}_i$ and the allocated demand volume m_i:

$$f(\mathbf{x}_i, m_i) = k(\mathbf{x}_i) + a(\mathbf{x}_i) m_i + b(\mathbf{x}_i) m_i^{\alpha}, \quad for \quad i = 1, 2, ..., n \tag{2}$$

where $k(\mathbf{x}_i)$ is the annualized fixed cost of the capacity acquisition cost. The coefficients $a(\mathbf{x}_i)$ and $b(\mathbf{x}_i)$ are both the annualized variable capacity acquisition cost per unit demand. Exponent α represents the economies ($0 < \alpha < 1$) or diseconomies ($\alpha > 1$).

3.4 Transportation cost

The LCAP aims to reasonably locate a set of new facilities to meet the demands of customers in the market region M. Distribution in each service region R_i is based on the direct shipping where each customer receives a single delivery. Let $d(\mathbf{x}_i, \mathbf{x}_j)$ denote the distance between $\mathbf{x}_i$ and $\mathbf{x}_j$ based on the Euclidean metric. We assume that the transportation cost between $\mathbf{x}_i$ and $\mathbf{x}_j$ in the market region can be approximated by $\varphi(\mathbf{x}_i, \mathbf{x}_j) = \Phi(d(\mathbf{x}_i, \mathbf{x}_j))$. Consequently, the transportation cost (or distance cost) $C_i = C(\mathbf{x}_i, R_i)$ of the facility located at $\mathbf{x}_i$ and assigned service region R_i in our model is formulated as follow:

$$C(\mathbf{x}_i, R_i) = \int_{R_i} \rho(\mathbf{x}) \varphi(\mathbf{x}_i, \mathbf{x}_j) d\mathbf{x} \tag{3}$$

Previous studies focus on the linear relationship between the transportation cost and the Euclidean distance, that is, $\Phi(d(\mathbf{x}_i, \mathbf{x}_j)) = Ad(\mathbf{x}_i, \mathbf{x}_j) + B$, where A and B are constants. However, Iri et al. [4] introduce that a customer in the service region R_i would enjoy a service of the i-th facility and the cost for him to get access to the facility can be expressed as a function (ordinarily, monotone increasing, and even convex) of the Euclidean distance. Therefore, the complexity of the urban traffic and the physical power of people are taken into account in our model, and we assume that the relationship between transportation cost and the Euclidean distance is non-linear. For simplification, the transportation cost is defined as follow:

$$\varphi(\mathbf{x}_i, \mathbf{x}_j) = \Phi(d(\mathbf{x}_i, \mathbf{x}_j)) = c\|\mathbf{x}_i - \mathbf{x}_j\|^2 \tag{4}$$

where $\|\mathbf{x}_i - \mathbf{x}_j\| = \sqrt{(x_i - x_j)^2 + (y_i - y_j)^2}$ represents the Euclidean distance, and c is a constant coefficient used to describe the transportation cost per unit. With Eq. (4), we can observe that the transportation cost per unit increases with the increasing of the Euclidean distance under the complex external situations. Consequently, the transportation cost $C(\mathbf{x}_i, R_i)$ of the i-th facility in the market region M can be reformulated as follow:

$$C(\mathbf{x}_i, R_i) = c \int_{R_i} \rho(\mathbf{x}) \|\mathbf{x}_i - \mathbf{x}_j\|^2 d\mathbf{x} \tag{5}$$

3.5 Simplification

In what follows, we simplify the LCAP based on some assumptions, and the model in Eq. (1) is reformulated as a multi-facility problem, so that it can be solved in an iteration way. We assume that the number of facilities is an exogenous decision, that is, the number of facilities is preseted in our model. Based on the simplification in [5], we select $F(\mathbf{x}_i) = F, k(\mathbf{x}_i) = k, a(\mathbf{x}_i) = a$, and $b(\mathbf{x}_i) = b$, whereas F, k, a, and b are constants. Furthermore, the LCAP is to locate a set of new facilities to meet the demands of customers in the market region M, and the sum of customers' demands in all service regions is equal to the demand volume of the whole market region M:

$$\sum_{i=1}^{n} m_i = \int_M \rho(\mathbf{x}) d\mathbf{x} \tag{6}$$

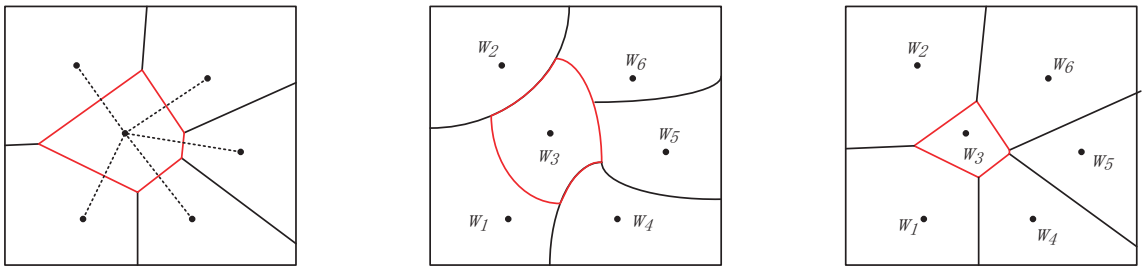

Fig. 1 Three allocation strategies based on geometric structure. The dots represent the location of facilities, w_i show the weighting coefficients, and the facet formed by red segments denote the allocation decision of the corresponding facility. (a) ordinary Voronoi diagram; (b) multiplicatively weighted Voronoi diagram; and (c) power diagram.

Accordingly, we can simplify the LCAP and further reformulate the model in Eq. (1) as:

$$\begin{aligned} &\min_{\mathbf{X},\mathbf{R}} E_{LCAP} = \sum_{i=1}^{n} \{bm_i^{\alpha} + c \int_{R_i} \rho(\mathbf{x}) \|\mathbf{x}_i - \mathbf{x}_j\|^2 d\mathbf{x}\} \\ &where \quad m_i = \int_{R_i} \rho(\mathbf{x}) d\mathbf{x} \end{aligned} \tag{7}$$

The first term in Eq. (7) is called the capacity acquisition cost, whereas the second term is represented as the transportation cost between customers and facilities. The simplified term in Eq. (1) is reformulated as the fixed cost. As we know, due to the joint location and allocation decisions, the LCAP is non-convex, which can hardly be solved. In the next section, we propose an iterative method for solving the LCAP.

4 Methodology

We now introduce the allocation method and present an equivalent formulation. Furthermore, an iterative method is proposed for solving the LCAP.

4.1 Allocation method

As mentioned above, both the location and allocation decisions are strategic decisions in the LCAP. Previous studies focus on the allocation decisions based on the Euclidean distance between customers and facilities, such as delivery services and door-to-door services, in which Voronoi diagrams are used to investigate the properties of allocation decisions [4]. Based on the Voronoi diagram, the allocation decisions are determined according to the following definition:

$$R_i = \{\mathbf{x} \in M | \ \|\mathbf{x} - \mathbf{x}_i\| \leq \|\mathbf{x} - \mathbf{x}_j\|, \ \forall j \neq i\} \tag{8}$$

However, there are some situations where the Euclidean distance cannot well express the attraction process of each facility, such as the retail store locating. In addition to the distance, the attraction of facilities depends on a set of features, such as the scale and service level of facilities, which are characterized by the weighting coefficients $\mathbf{W} = \{w_i\}_{i=1}^n$ [7]. For instance, the larger scale and the higher service level of facility, the greater the weighting coefficient, which means that more customers will be attracted, and the larger service region will be assigned to it. Some weighted Voronoi diagrams [23] can be more useful for identifying and characterizing these features, such as multiplicatively weighted Voronoi diagrams, as shown in Fig. 1(b). A set of weighting coefficients $\mathbf{W} = \{w_i\}_{i=1}^n$ (also called "weights"), are applied in these diagrams, such that the service region R_i increases with the weight w_i. Note that the weighted Voronoi diagrams will degenerate to the ordinary Voronoi diagram when all the weights are equal [24]. In addition, as shown in Fig. 1(b), the service region R_i defined by the bisector between $\mathbf{x}_i$ and $\mathbf{x}_j$ may be non-convex, which may result in holes in the optimization process [25], that is, there may be some customers having no facility to provide services for them. Furthermore, more time consumption is required for computing the multiplicatively weighted Voronoi diagram.

As an extension of Voronoi diagrams, power diagrams [23] play an essential role in solving this problem, as shown in Fig. 1(c). An important characteristic of power diagrams is that the resulting partitions are always convex, and the bisectors are straight lines. Furthermore, power diagrams have the characteristics of precise capacity constraints. Therefore, the allocation decisions are determined based on the power diagrams as follow:

$$R_i = \{\mathbf{x} \in M | \ \|\mathbf{x} - \mathbf{x}_i\|^2 - w_i \leq \|\mathbf{x} - \mathbf{x}_j\|^2 - w_j, \ \forall j \neq i\} \tag{9}$$

Consequently, the strategic decisions based on the power diagram are actually the facility locations and weighting coefficients (or "weights") decisions.

4.2 Power diagram-based iterative method

We apply the power diagrams to determine the allocation decisions in this paper, where the weighting coefficients $\mathbf{W} = \{w_i\}_{i=1}^n$ characterize the attraction of facilities. First of all, we present some definitions and concepts here. Let $\mathbf{X} = \{\mathbf{x}_i\}_{i=1}^n$ denote the location of facilities to be located in the market

region M, $\mathbf{R} = \{R_i\}_{i=1}^n$ are the service regions allocated to facilities. Assume that the population distribution (or demand distribution) in the market region can be represented by a density function $\rho(\mathbf{x})$, and the total demand of service region R_i is m_i. Additionally, e_{ij} denotes the regular edge between two adjacent facilities $\mathbf{x}_i$ and $\mathbf{x}_j$. e_{ij}^* represents the dual edge separating the service regions R_i and R_j, and Ω_i denotes the set of facilities adjacent to the i-th facility. Fig. 2 illustrates a power partition of a rectangle market region with ten facilities. From the results we observe $\Omega_4 = \{1, 2, 3, 5, 6, 8\}$, and $\Omega_6 = \{3, 4, 7, 8, 10\}$.

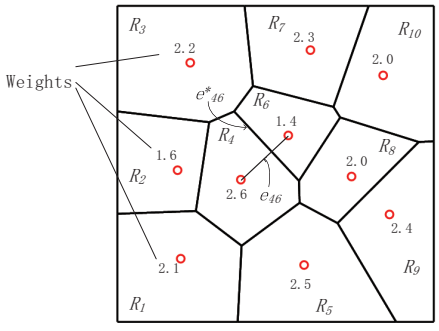

Fig. 2 Service regions of ten facilities based on power diagrams.

As soon as the location decisions and weights are decided, the solutions can be easily obtained. In this paper, an effectively iterative method is introduced, where two key operations are: (1) finding the optimal weights $\mathbf{W}$ of facilities using the gradient descent method; and (2) employing Lloyd's method to optimize the location $\mathbf{X}$ of facilities.

4.2.1 Weight optimization

In what follows, we analyze the optimization process of weights of facilities when the location of each facility is given. When the location of each facility is fixed, the optimization process of weights of facilities can be considered as a univariate function optimization process. We provide an equivalent formulation of Eq. (7) as follow:

$$\begin{aligned} &\min_{\mathbf{W}} E_{LCAP} = \sum_{i=1}^{n} bm_i^{\alpha} + c\int_{R_i} \rho(\mathbf{x})\|\mathbf{x} - \mathbf{x}_i^*\|^2 d\mathbf{x} \\ &s.t.\ \ \mathbf{x}_i^* = \arg\min_{\mathbf{x}_i}\{bm_i^{\alpha} + c\int_{R_i} \rho(\mathbf{x})\|\mathbf{x} - \mathbf{x}_i\|^2 d\mathbf{x}\} \end{aligned} \tag{10}$$

As mentioned above, given the location of each facility, the LCAP aims to find the weights of facilities to minimize the total cost in Eq. (10). We adopt the gradient descent method to update the weights of facilities, in which the backtracking line search method is applied to compute the optimal step size to minimize the total cost. To this end, we derive the gradient of the total cost in Eq. (10). According to the general Leibniz rule [26], the derivation of the total cost E_{LCAP} *w.r.t.* weight w_i of facility i can be computed as follow:

$$\nabla_{w_i} E_{LCAP} = \sum_{j\in\Omega_i} [\alpha b(m_j^{\alpha-1} - m_i^{\alpha-1}) + c(w_j - w_i)]\nabla_{w_i} m_j \tag{11}$$

As described in [27], the derivation $\nabla_{w_i} m_j$ can be computed as follow:

$$\nabla_{w_i} m_j = -\frac{\bar{\rho}_{ij}}{2} \cdot \frac{|e_{ij}^*|}{|e_{ij}|} \tag{12}$$

where the average value of the field $\rho(\mathbf{x})$ over e_{ij}^* is referred as $\bar{\rho}_{ij}$. The gradient of the total cost E_{LCAP} with respect to w_i is provided in the appendix A.

4.2.2 Location optimization

Given a set of service regions, the LCAP can be reduced to the p-median problem, which locates a set of facilities to minimize the total cost between customers and facilities. Existing studies have been conducted to solve the p-median problem, and indicate that the transportation cost is minimized when each facility is located at the mass center of the corresponding service region [28]. In this paper, Lloyd's method is employed to optimize the location of each facility, that is, the location of facility i is moved to the mass center $\tilde{\mathbf{x}}_i$ of the service region R_i according to the following term:

$$\tilde{\mathbf{x}}_i = \frac{\int_{R_i} \mathbf{x}\rho(\mathbf{x})d\mathbf{x}}{\int_{R_i} \rho(\mathbf{x})d\mathbf{x}} \tag{13}$$

4.2.3 Iterative algorithm

Algorithm 1 Iterative algorithm for solving the LCAP

Input: the market region M, demand density function $\rho(\mathbf{x})$, the number of facilities n, and a threshold ϵ as the termination

Output: $(\mathbf{X}, \mathbf{R})$

1: **Initialization:** set $k = 0$, $\mathbf{X}^{(0)}$ to be n randomly generated sites, and $\mathbf{W} = \mathbf{0}$
2: **repeat**
3: Compute the gradient $\nabla_{w_i} E_{LCAP}$ in Eq. (11)
4: Estimate the step-size Δt for updating $\mathbf{W}$ by the backtracking line search method
5: $w_i = w_i + \Delta t \cdot \nabla_{w_i} E_{LCAP}$
6: Compute the mass centers $\tilde{\mathbf{x}}$ of service regions based on Eq. (13)
7: Move the facilities to their respective mass centers using Lloyd's method
8: $k = k + 1$
9: Compute the total cost $E_{LCAP}^{(k)}$ in Eq. (10)
10: **until** $\frac{|E_{LCAP}^{(k)} - E_{LCAP}^{(k-1)}|}{E_{LCAP}^{(k-1)}} < \epsilon$

Consequently, our method works as shown in Fig. 3. Firstly, we start from a feasible location $\mathbf{X}^{(0)}$ randomly generated in

the market region M, and the weights $\mathbf{W}^{(0)}$ of all facilities are set to be equal. Assuming $\mathbf{X}^{(k)}$, the position in the k-th iteration, is a feasible location as well, and $\mathbf{W}^{(k)}$ is the weights in the k-th iteration. Next, we compute the reduced-gradient vector based on Eq. (11) and feed it to the backtracking line seach solver to update $\mathbf{W}^{(k)}$ to $\mathbf{W}^{(k+1)}$. Meanwhile, Lloyd's method is applied to update $\mathbf{X}^{(k)}$ to $\mathbf{X}^{(k+1)}$ based on Eq. (13). Thus, the $(k+1)$-th iteration yields the next position $\mathbf{X}^{(k+1)}$ and weights $\mathbf{W}^{(k+1)}$. The iterative process is repeated until the termination condition is satisfied. The pseudocode of our method is given in algorithm 1.

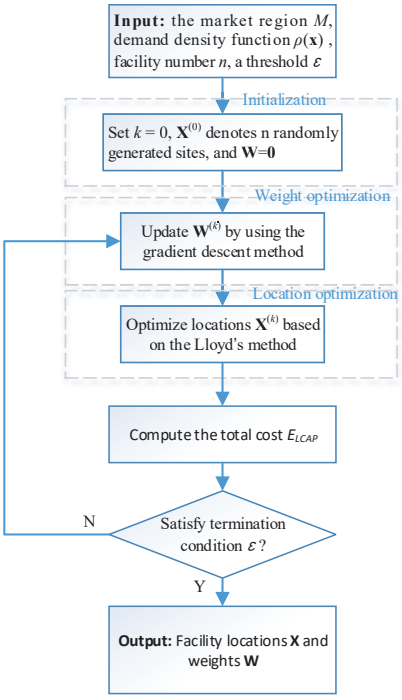

Fig. 3 Overview of our iterative algorithm.

4.3 Step size revision

In the above, the gradient descent method is used for updating the weights of facilities, where the backtracking line search method is applied to find the optimal step size to minimize the total cost. However, in the line-search process, the impact of excessive step size on the power diagram construction is ignored. The service region of some facilities may be empty when the step size is too large. As shown in Fig. 4, there are five points representing the retail stores. Each retail store has associated features, represented by the weight. The computation result of the service region R_i with appropriate w_k is demonstrated in Fig. 4(a), while Fig. 4(b) shows the computation result with inappropriate w_k.

There may be some empty service regions in the power diagram construction when using the backtracking line search method to find the optimal step size to minimize the total cost. To solve this issue, the too large step size is revised in our method as follow:

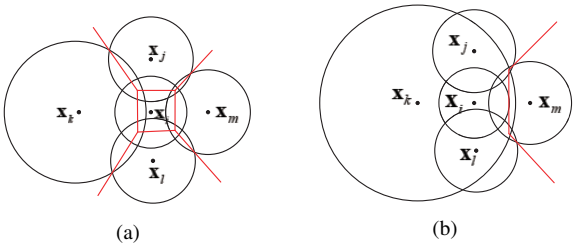

Fig. 4 Computation of the service region R_i with different weight w_k. (a) appropriate weight w_k; (b) inappropriate weight w_k.

$$\Delta w_i = \Delta t' \cdot \nabla_{w_i} E_{LCAP} = \beta \cdot \Delta t \cdot \nabla_{w_i} E_{LCAP} \tag{14}$$

where $0 < \beta < 1$ is the adjustment ratio, Δt represents the original step size found by the backtracking line search method, and $\Delta t'$ denotes the revised step size. As we know, the empty service region is associated with the weights of the adjacent facilities in the process of constructing power diagrams. Therefore, the empty service region can be avoided by reducing the variance of the weights.

5 Experiments

In this section, we present the computational results to verify the efficiency of our proposed method, and investigate the influence of different parameters in our experiments. We implement our algorithm in C++, and all the experiments are performed on a computer with 3.6 GHz Inter(R) Core (TM) i7-9700K CPU and 16GB memory.

Based on the description in [5, 6], the market region M is selected as a squared service region with a side length of 1, and the coefficient b is set to 0.5. Three types of demand densities are considered in our experiments: uniform (UD), linear (LD), and non-linear (NLD) demand densities. It is worth noting that Gaussian demand density is a special case of non-linear demand density, as illustrated in Fig. 5. The number of facilities to be located in the market region is chosen from the set $\{2, 3, ..., 16\}$. The default value of the exponent α is 0.5, and the default value of the parameter c is set to 100. The threshold value ϵ is fixed at 10^{-5}. To study the effect of different values of parameters on the results, the above-mentioned default values are allowed to alter as $\alpha \in \{0.5, 1, 2\}$, and $c \in \{75, 100, 125\}$ in our experiments.

It is worth mentioning that the total demand in the market region may be different with various demand densities. To ensure the consistency of the experiments, the demand of each service region is replaced with the percentage of the total demand of the market region.

5.1 Computational performance

Since the gradient descent method is used to update the weight of each facility, the numerical tolerance parameter is critical for computational performance. We first test the effect of

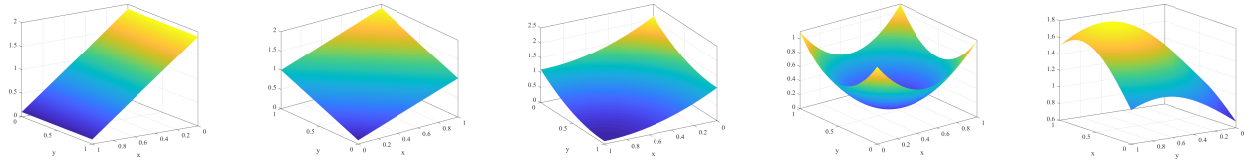

(a) LD-1 (b) LD-2 (c) NLD-1 (d) NLD-2 (e) Gaussian

Fig. 5 Linear and non-linear demand density functions used in our experiments. (a)$\rho(x, y) = 0.1+1.8x$; (b)$\rho(x, y) = 1.8-0.9x-0.9y$; (c)$\rho(x, y) = 0.1+x^2+y^2$; (d)$\rho(x, y) = 0.1 + 2 \times [(x - 0.5)^2 + (y - 0.5)^2]$; and (e)$\rho(x, y) = 1.8 \times e^{-[(x-0.3)^2+(y-0.3)^2]}$.

threshold value ϵ on the computational performance, which is related to the computation accuracy of the proposed algorithm. Table 2 illustrates the number of iterations and the computational time of the LCAP with $n = 10$, and demand density LD-1, where other parameters are set to the default values. In our implementation, we start with an initial tolerance of 10^{-2} and reduce it gradually as needed. The threshold value, shown in the second column, denotes the tolerance parameter set in the gradient descent method. The last column represents the actual accuracy, which is defined as follow:

$$Actual \quad accuracy = \frac{|E^{(k)}_{LCAP} - E^{(k-1)}_{LCAP}|}{E^{(k-1)}_{LCAP}}$$

Table 2 Effect of numerical tolerance on the computational performance ($n = 10$, and LD-1).

Case no	ϵ	Iterations	Total time (s)	Actual accuracy
1	1.00E-02	8	0.124	8.98E-03
2	1.00E-03	18	0.307	8.34E-04
3	1.00E-04	28	0.477	8.53E-05
4	1.00E-05	36	0.619	7.92E-06
5	1.00E-06	79	2.819	9.97E-07
6	1.00E-07	230	6.220	9.99E-08

We then analyze the effect of various demand densities and the number of facilities on the computational performance. For the demand densities, we experiment with three types of demand densities: uniform (UD), linear (LD) and non-linear (NLD) demand densities, as shown in Fig. 5. Fig. 6 illustrates the computational time for six demand densities and three different numbers of facilities ($n = 4$, 8, and 12). The threshold value ϵ is fixed at 10^{-5} in this experiment.

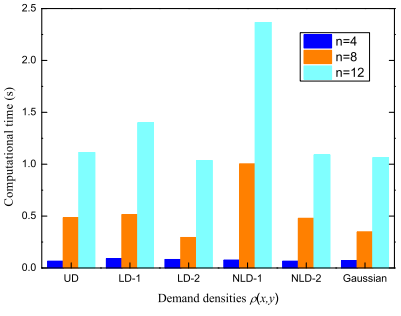

Fig. 6 Computational time with various demand densities.

From the results in Table 2 and Fig. 6, we can observe that the threshold value plays an essential role in the computational performance. The number of iterations and computational time increase with the threshold value reducing. For instance, when the threshold value is less than 10^{-7}, there are hundreds of iterations to be conducted in the iterative algorithm. Furthermore, the computational performance is also affected by the number of facilities. When the number of facilities increases, the computational time of the iterative algorithm increases, accordingly. Besides, the computational results in Fig. 6 demonstrate that demand densities have significant impact on the computational time of our proposed method. Much more time consumption is required for the LCAP with complex demand densities, as compared to simple demand densities.

5.2 Analysis

5.2.1 Result analysis

In this section, a comprehensive set of computational experiments are conducted to verify the effectiveness of our proposed method. Based on the results of a set of preliminary experiments, the optimal values for the fixed cost of a single facility is set to 0.15 in our experiments. Table 3 illustrates the computational results of the LCAP with uniform demand density. In our experiment, the exponent α is 0.5, and the coefficient c is set to 100. The first column "n" shows the number of facilities to be located. The column "CAC" denotes the capacity acquisition cost as the objective function. The transportation cost (TC) and fixed cost (FC) are reported in columns "TC" and "FC", respectively. The column "SC" represents the total cost (the sum of CAC, TC, and FC). The last two columns, labeled as "CAC%" and "TC%", denote the percentage of the corresponding cost. Furthermore, for every solution obtained by our proposed method and reported in Table 2, we plot the location of facilities in the market region along with the corresponding power partitions, and depict the resulting layouts in Fig. 7.

From Table 2 and Fig. 7, we can observe that when the number of facilities is small, the transportation cost has a larger of the total cost, whereas the capacity acquisition cost and fixed cost have a smaller share. In other words, more material resources will be consumed on delivery. Note that, as the number of facilities increases, the transportation cost reduces, while the fixed cost and the capacity acquisition cost

Table 3 Computational results of the LCAP with uniform demand density.

n	CAC	TC	FC	SC	CAC%	TC%
2	0.707	10.418	0.300	11.425	6.19%	91.18%
3	0.865	6.618	0.450	7.933	10.90%	83.42%
4	1.000	4.167	0.600	5.767	17.34%	72.26%
5	1.115	3.551	0.750	5.416	20.59%	65.56%
6	1.219	3.049	0.900	5.168	23.59%	59.00%
7	1.321	2.564	1.050	4.935	26.77%	51.96%
8	1.413	2.165	1.200	4.778	29.57%	45.31%
9	1.500	1.852	1.350	4.702	31.90%	39.39%
10	1.579	1.706	1.500	4.785	33.00%	35.65%

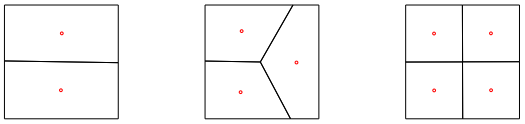

(a) $n = 2$ (b) $n = 3$ (c) $n = 4$

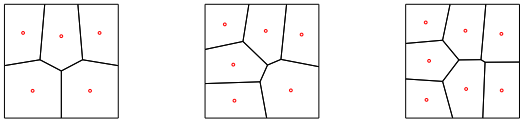

(d) $n = 5$ (e) $n = 6$ (f) $n = 7$

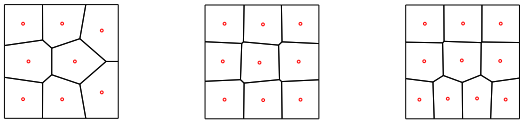

(g) $n = 8$ (h) $n = 9$ (i) $n = 10$

Fig. 7 Computational results for different numbers of facilities.

get larger.

5.2.2 Exponent analysis

According to the economies of scale theory, different values of exponent α represent the economies ($0 < \alpha < 1$) or diseconomies ($\alpha > 1$) of scale. The capacity acquisition cost varing different values of α is presented in Fig. 8(a), where the slope of the capacity acquisition cost curve represents the capacity acquisition cost per unit. It can be observed that the capacity acquisition cost per unit gradually decreases under economies of scale, while increasing under diseconomies of scale.

We study the impact of the exponent α on the computational results. In our experiment, 15 facilities will be located in the market region M, where customers are evenly distributed. The value of exponent α is set to $\alpha \in \{0.5, 1.0, 2.0\}$, and other parameters are set to the default values. Fig. 8(b-d) show the resulting layouts with different values of exponent α, where the red dots denote the location of facilities.

Specially, under the diseconomies of scale ($\alpha > 1$), the capacity acquisition cost is minimal when the capacities of facilities are equal, and the optimal solution can be obtained when facilities are located at their respective mass centers. However, the value of exponent α is set to 1.0, which means that the first term in Eq. (7) is a fixed value. The LCAP

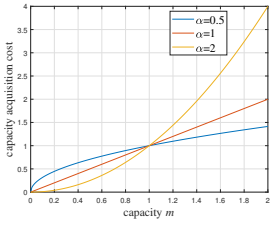

(a) cost curves

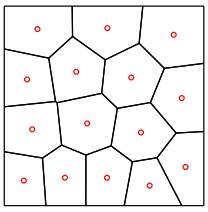

(b) $\alpha = 0.5$

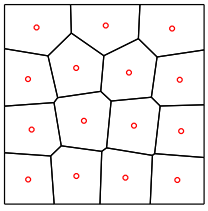

(c) $\alpha = 1.0$

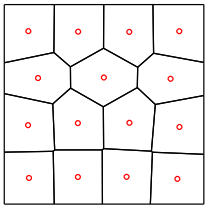

(d) $\alpha = 2.0$

Fig. 8 Computational results with different values of exponent α.

degenerates to a p-center problem, and it can be solved by Lloyd's method.

As the results shown in Fig. 8, we can observe that there are certain differences in facility location and allocation decisions under different economies models. As mentioned above, the optimal solution in Fig. 8(d) should be that the capacities of facilities are equal, and the location of each facility is at its mass center. According to our calculations, the capacity error between the solution obtained by our algorithm and optimal solution is no more than 2%.

5.2.3 Parametric analysis

As we all know, the transportation cost per unit in different regions varies greatly. For instance, the price per kilometer for taking a taxi is much higher in first-tier city than in other cities. We study the effect of two other input parameters, namely the demand density $\rho(\mathbf{x})$ and the coefficient c. To this end, some experiments are further conducted by taking the default value as the input for other coefficients (i.e. $\alpha = 0.5$). The coefficient c is set to $c \in \{75, 100, 125\}$, and the above-mentioned three types of demand density functions are also taken into consideration in this experiment. Fig. 9 illustrates the total cost for varying numbers of facilities with different demand densities with three different values of c. The final layout configurations for different demand densities are shown in Fig. 10 for the LCAP with 12 facilities. Four demand densities are used, including the linear (LD-1, LD-2) and non-linear (NLD-1, NLD-2) demand densities.

As shown in Fig. 9-10, larger transportation cost result in substantially higher total cost as the transportation cost increases with larger value of c. As mentioned above, an increasing number of facilities will lead to smaller transportation cost, and larger capacity acquisition cost. Thus, when the number of facilities exceeds a threshold (i.e. $n = 8$ in Fig. 9),

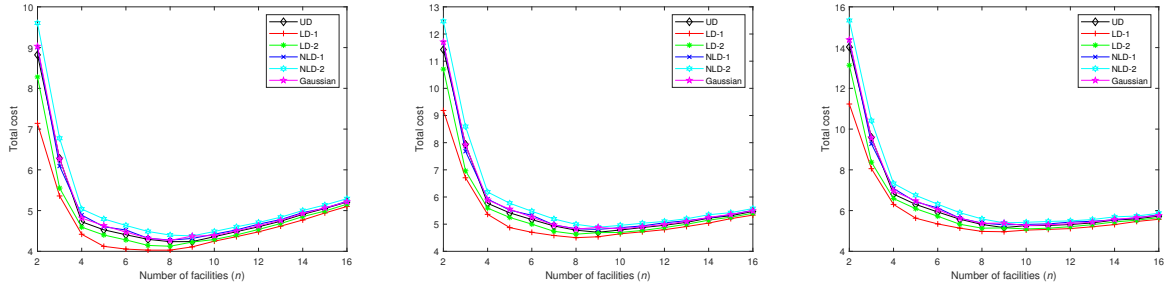

(a) $c = 75$ (b) $c = 100$ (c) $c = 125$

Fig. 9 Total cost curves with different values of c and various demand densities.

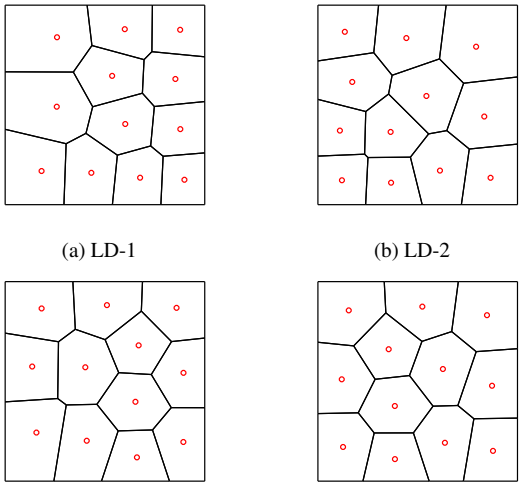

(a) LD-1 (b) LD-2

(c) NLD-1 (d) NLD-2

Fig. 10 Results for 12 facilities with various demand densities.

the total cost of the facility location and capacity acquisition cost will gradually increase. Meanwhile, both the total cost and the layout result are affected by different demand densities. The LCAP with NLD-2 has the largest total cost, while gets the lowest with LD-1.

5.3 Comparison

To further evaluate our proposed method, we compare the experimental results obtained by our proposed method with those obtained by other methods proposed by Iri [4], Murat [5], and Bourne [6]. To maintain consistency in the experiment, the squared region is selected as the default market region. Additionally, the number of facilities is 16, and the threshold value ϵ is fixed at 10^{-5}. The computational time of the LCAP obtained by our proposed method and other methods are reported in Table 4, where $\alpha = 0.5$ in our proposed method, $a = 1.0$ in the method proposed by Murat [5], and $\lambda = 0.5$ in the method proposed by Bourne [6]. Furthermore, three demand densities are considered, and they are uniform demand density (UD), linear demand density (LD-1) and non-linear demand density (NLD-1).

It should be mentioned that the capacity acquisition cost is not considered in [4], which is considered in other methods. Besides, it is assumed that capacity acquisition cost can be approximated with a linear function in [5]. With Eq. (6), we can observe that the capacity acquisition cost in the market region M is a fixed value. Bourne et. al [6] aim to solve the LCAP with uniform demand density. Furthermore, the relationship of transportation cost and the Euclidean distance is linear in [5], while non-linear in other methods.

Table 4 Performance comparison to other methods with various demand densities (in seconds).

Methods	Allocation strategy		Demand densities		
	VD[1]	PD[2]	UD	LD-1	NLD-1
Iri et al. [4]	✓		4.230	4.536	4.457
Murat et al. [5]	✓		99.890	115.24	103.75
Bourne et al. [6]		✓	3.321	/	/
Proposed method		✓	2.198	2.199	2.538

[1] VD: Voronoi diagram [2] PD: power diagram

To illustrate the difference between the linear and non-linear relationship of the transportation cost and the Euclidean distance, the solutions of the LCAP obtained by the method proposed by Murat et al. [5] and our proposed method are presented in Fig. 11, where all parameters are set to the default values in our method. The blue as well as red dots represent the location of facilities, and each facet formed by segments denotes the service region assigned to the corresponding facility. Furthermore, the total distance (TD) is computed as follow:

$$TD = \sum_{i=1}^{n} \int_{R_i} \rho(\mathbf{x}) \|\mathbf{x} - \mathbf{x}_i\| d\mathbf{x} \tag{15}$$

From Table 4 and Fig. 11, we can observe that our method outperforms other methods. Much more time consuming is required to solve the LCAP in other methods as compared with our proposed methods. The high efficiency of our method due to the steepest descent method based on the weights, instead of the vertices in the method proposed in [5]. Furthermore, the non-linear relationship of the transportation cost and the Euclidean distance in the multi-facility location and capacity acquisition problem may effectively reduce the total distance, and the solutions obtained by our method is more symmetrical.

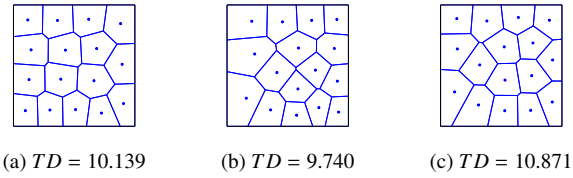

(a) TD = 10.139 (b) TD = 9.740 (c) TD = 10.871

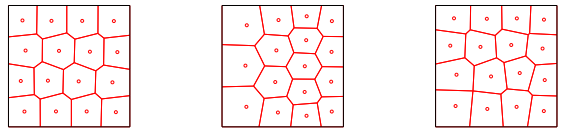

(a) TD = 9.924 (b) TD = 9.382 (c) TD = 10.694

Fig. 11 Solutions obtained by the method proposed by Murat et al. [5] and our proposed method. The first row: solutions obtained by the method proposed in [5]. The second row: solutions obtained by our proposed method. The first column: uniform demand density (UD). The second column: linear demand density (LD-1). The third column: non-linear demand density (NDL-1).

5.4 More results

We conduct experiments under three different market regions to verify the versatility of our proposed method. In our experiments, the market region is set as triangle region, convex region, and star region. Note that, the demands of customers in these regions are approximately set to 1. For simiplification, the uniform demand density (UD) is selected, and the number of facilities is fixed at 16, while other input parameters are set to the default values. Fig. 12 illustrates the results of the LCAP for various market regions, which demonstrate that our algorithm can be applied to more complex market regions.

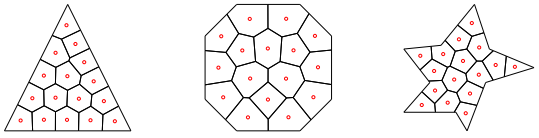

(a) triangle region (b) convex region (a) star region

Fig. 12 Results of the LCAP with various market regions.

To further illustrate the feasibility of our proposed method in practice, 25 emergency centers are to be located in a certain city, and we minimize the total cost on the premise that all personnel are served. First of all, we collect census data online to obtain sample data, and map these sample data to a squared area with a side length of 1. Then, the Newling model [29] is adopted to simulate the population density of this city. The population density function is shown in Fig. 13(a), and the Newling model function is:

$$\rho(x,y) = 5.858 \times e^{-5\times[(x-\frac{19}{50})^2+(y-\frac{35}{50})^2]-0.05\times[(x-\frac{19}{50})^2+(y-\frac{35}{50})^2]^{\frac{1}{2}}} \tag{16}$$

It should be mentioned that the exponent α and the coefficient c are set to the default values. Based on the optimal solution obtained by our proposed method, the final layout configuration of 25 emergency centers is presented in Fig.

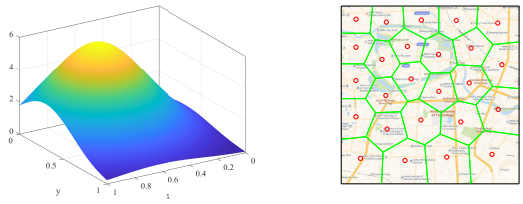

(a) demand density (b) layout result

Fig. 13 The layout of 25 emergency centers.

13(b). The red dots denote the location of facilities, and facets formed by green segments represent the service regions of facilities. The result in Fig. 13 proves that our proposed method can effectively solve the actual locating problems.

6 Conclusion

In this paper, we propose a continuous model for the facility location and capacity acquisition problem with dense demand. Various demand densities are employed to adapt to the population distribution in the market region. A set of weighting coefficients are used to characterize the features of facilities, which represent the attracting process of each facility. To this end, the power diagrams are applied to determine the allocation decisions, and a power diagram based iterative method for solving the facility location and capacity acquisition problem with dense demand is developed. A comprehensive set of computational experiments are conducted to verify the effectiveness of our proposed method.

Limitation and future work. The capacity of each facilities is unlimited in our proposed method, and it has a wide range of options. However, in practical applications, the capacity of each facilities may be subject to some constraints, such as interval constraints, or partial fixed value constraints. In future work, we will extend our proposed method to a more general version.

Acknowledgements This study was partially supported by the National Natural Science Foundation of China (Grant No. 61972128).

Appendixes

Appendix A The derivation of the total cost

In this section, we provide the derivation of the total cost E_{LCAP} with respect to the weights in Eq. (10) in the main text.

Notion: We denote the regular edge between two adjacent facilities $\mathbf{x}_i$ and $\mathbf{x}_j$ by e_{ij}, the dual edge separating the service regions R_i and R_j by e^*_{ij}, and Ω_i denotes the neighbor facilities of $\mathbf{x}_i$.

Total cost: We now define the total cost in Eq. (10) as follow:

$$E_{LCAP} = \sum_{i=1}^{n} bm_i^{\alpha} + c\int_{R_i} \|\mathbf{x}-\mathbf{x}_i\|^2\rho(\mathbf{x})d\mathbf{x}$$
$$\text{where } m_i = \int_{R_i}\rho(\mathbf{x})d\mathbf{x} \tag{17}$$

Derivation of w_i: We now provide the derivation of the total cost E_{LCAP} with respect to w_i:

$$\begin{aligned}\nabla_{w_i}E_{LCAP} &= b(\alpha m_i^{\alpha-1}\cdot\nabla_{w_i}m_i + \sum_{j\in\Omega_i}\alpha m_j^{\alpha-1}\cdot\nabla_{w_i}m_j)\\ &+ c\cdot\sum_{j\in\{i\}+\Omega_i}\int_{\partial R_i}\rho(\mathbf{x})\|\mathbf{x}-\mathbf{x}_i\|^2\cdot(\nabla_{w_i}\mathbf{x}\cdot\mathbf{n})d\mathbf{x}\\ &= \sum_{j\in\Omega_i}[\alpha b(m_j^{\alpha-1}-m_i^{\alpha-1})]\nabla_{w_i}m_j\\ &+ c\cdot\sum_{j\in\Omega_i}\int_{e_{ij}^*}\rho(\mathbf{x})(\|\mathbf{x}-\mathbf{x}_j\|^2-\|\mathbf{x}-\mathbf{x}_i\|^2)(\nabla_{w_i}\mathbf{x}\cdot\frac{\mathbf{x}_i-\mathbf{x}_j}{|e_{ij}|})d\mathbf{x}\end{aligned} \tag{18}$$

where ∂R_i is the boundary of R_i, and $\mathbf{n}$ is the outward unit norm vector on the boundary R_i. Based on the envelope theorem, we have

$$\nabla_{w_i}\mathbf{x}\cdot\mathbf{n} = \nabla_{w_i}\cdot\frac{\mathbf{x}_i-\mathbf{x}_j}{|e_{ij}|} = \frac{1}{2|e_{ij}|},\quad \forall\mathbf{x}\in e_{ij}^* \tag{19}$$

Hence, the derivation of E_{LCAP} with respect to w_i can be computed according to the derivations above:

$$\nabla_{w_i}E_{LCAP} = \sum_{j\in\Omega_i}[\alpha b(m_j^{\alpha-1}-m_i^{\alpha-1}) + c(w_j-w_i)]\nabla_{w_i}m_j \tag{20}$$

Appendix B The computational time in Section 5.2

In this section, more computational time results are provided to verify the effectiveness of our proposed method.

Table 5 presents the computational time for the LCAP with uniform dense demand under various number of facilities, which is the corresponding execution time of Table 3 and Fig. 7. Besides, the computational time for the LCAP with various values of α is shown in Table 6, which is the execution time of Fig. 8. Furthermore, the computational time curves with different number of facilities and various demand densities are introduced in Fig. 14, which represents the execution time of Fig. 9.

Table 5 Computational time for the LCAP with uniform dense demand (in seconds).

n	2	3	4	5	6	7	8	9	10
T(s)	0.043	0.057	0.064	0.127	0.229	0.294	0.484	0.691	0.802

*the corresponding computational time of Table 3 and Fig. 7.

Table 6 Computational time for the LCAP with various values of α (in seconds).

Results	Fig. 8(b) $n=15,\alpha=0.5$	Fig. 8(c) $n=15,\alpha=1.0$	Fig. 8(d) $n=15,\alpha=2.0$
T(s)	1.927	2.065	2.141

*the corresponding computational time of Fig. 8.

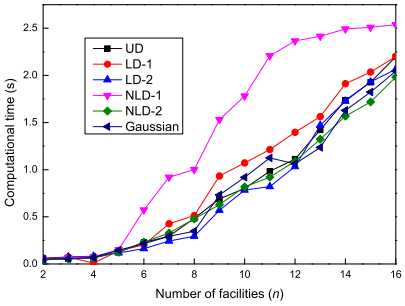

Fig. 14 computational time curves with different number of facilities and various demand densities

References

1. Cooper L. Location-allocation problems. Oper. Res., 1963, 11(3): 331–343
2. Fan Q, Ansari N. On cost aware cloudlet placement for mobile edge computing. IEEE/CAA Journal of Automatica Sinica, 2019, 6(4): 926–937
3. Wu P, Yang C H, Chu F, Zhou M, Sedraoui K, Al Sokhiry F S. Cost-profit trade-off for optimally locating automotive service firms under uncertainty. IEEE Transactions on Intelligent Transportation Systems, 2021, 22(2): 1014–1025
4. Iri M, Myrota K, Ohya T. A fast voronoi-diagram algorithm with applications to geographical optimization problems. In: Proceedings of the 11th IFIP Conference Copenhagen. 1983, 273–288
5. Murat A, Verter V, Laporte G. A continuous analysis framework for the solution of location–allocation problems with dense demand. Computers & Operations Research, 2010, 37(1): 123–136
6. Bourne D P, Peletier M A, Roper S M. Hexagonal patterns in a simplified model for block copolymers. SIAM Journal on Applied Mathematics, 2014, 74(5): 1315–1337
7. Novaes A G, Cursi d J S, Silva d A C, Souza J C. Solving continuous location–districting problems with voronoi diagrams. Computers & operations research, 2009, 36(1): 40–59
8. Fernández E, Hinojosa Y, Puerto J. Filtering policies in loss queuing network location problems. Annals of Operations Research, 2005, 136(1): 259–283
9. Lin C. Stochastic single-source capacitated facility location model with service level requirements. International Journal of Production Economics, 2009, 117(2): 439–451
10. Li S, Li X, Zhang D, Zhou L. Joint optimization of distribution network design and two-echelon inventory control with stochastic demand and co2 emission tax charges. PloS one, 2017, 12(1): 1–22
11. Ankrah R, Lacroix B, McCall J, Hardwick A, Conway A. Introducing the dynamic customer location-allocation problem. In: Proceedings of the 2019 IEEE Congress on Evolutionary Computation (CEC). 2019, 3157–3164

12. Zhou J, Liu B. Modeling capacitated location–allocation problem with fuzzy demands. Computers & industrial engineering, 2007, 53(3): 454–468
13. Marucheck A S, Aly A A. An efficient algorithm for the location-allocation problem with rectangular regions. Naval Research Logistics Quarterly, 1981, 28(2): 309–323
14. Wang Z. Two-stage facilities location-allocation problems with curved demands considered. In: Proceedings of the 16th International Conference on Service Systems and Service Management (ICSSSM). 2019, 1–5
15. Yin Y, Cao B. A genetic algorithm based approach for capacitated location/allocation problems. In: Proceedings of the 2011 International Conference on Electronics, Communications and Control (ICECC). 2011, 25–28
16. Harris I, Mumford C L, Naim M M. An evolutionary bi-objective approach to the capacitated facility location problem with cost and co2 emissions. In: Proceedings of the 13th annual conference on Genetic and evolutionary computation. 2011, 697–704
17. Liu H C, Yang M, Zhou M, Tian G. An integrated multi-criteria decision making approach to location planning of electric vehicle charging stations. IEEE Transactions on Intelligent Transportation Systems, 2018, 20(1): 362–373
18. Grine F Z, Kamach O, Sefiani N. A new efficient metaheuristic for solving the uncapacitated single allocation p-hub median problem. In: Proceedings of the 2018 International Colloquium on Logistics and Supply Chain Management (LOGISTIQUA). 2018, 69–74
19. Dasci A, Verter V. A continuous model for production–distribution system design. European Journal of Operational Research, 2001, 129(2): 287–298
20. Murat A, Laporte G, Verter V. A global shooting algorithm for the facility location and capacity acquisition problem on a line with dense demand. Computers & Operations Research, 2016, 71: 1–15
21. Turken N, Carrillo J, Verter V. Facility location and capacity acquisition under carbon tax and emissions limits: To centralize or to decentralize? International Journal of Production Economics, 2017, 187: 126–141
22. Joseph M, Wang F. Population density patterns in port-au-prince, haiti: A model of latin american city? Cities, 2010, 27(3): 127–136
23. Balzer M. Capacity-constrained voronoi diagrams in continuous spaces. In: Proceedings of the 6th International Symposium on Voronoi Diagrams. 2009, 79–88
24. Aurenhammer F. Power diagrams: properties, algorithms and applications. SIAM Journal on Computing, 1987, 16(1): 78–96
25. Okabe A, Suzuki A. Locational optimization problems solved through voronoi diagrams. European Journal of Operational Research, 1997, 98(3): 445–456
26. Flanders H. Differentiation under the integral sign. The American Mathematical Monthly, 1973, 80(6): 615–627
27. Xin S Q, Lévy B, Chen Z, Chu L, Yu Y, Tu C, Wang W. Centroidal power diagrams with capacity constraints: Computation, applications, and extension. ACM Transactions on Graphics (TOG), 2016, 35(6): 1–12
28. Brimberg J, Salhi S. A continuous location-allocation problem with zone-dependent fixed cost. Annals of Operations Research, 2005, 136(1): 99–115
29. Newling B E. The spatial variation of urban population densities. Geographical Review, 1969, 242–252